Article

Cell

Targeting of Fn14 Prevents Cancer-Induced Cachexia and Prolongs Survival

Graphical Abstract

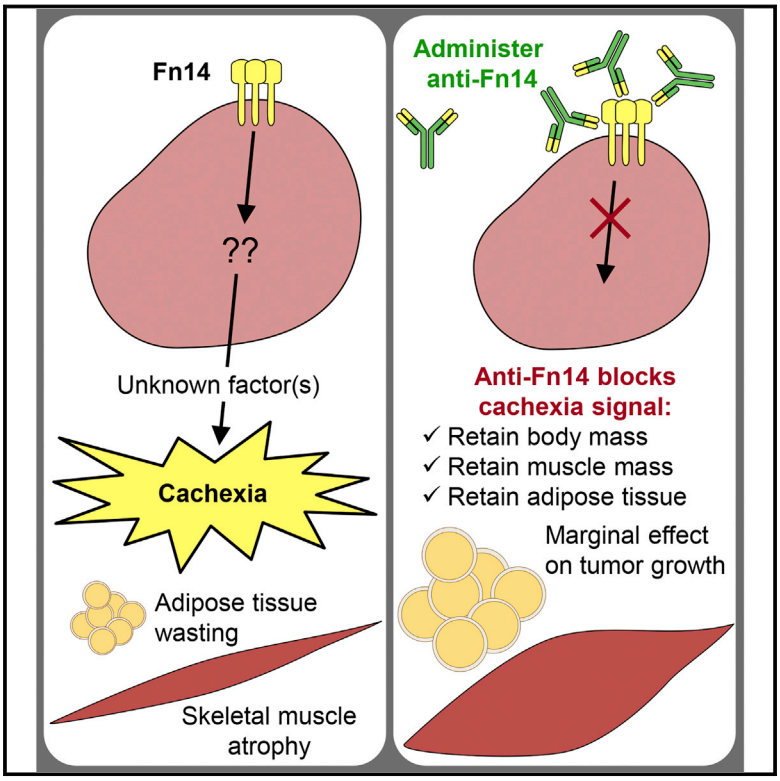

Authors

Amelia J. Johnston, Kate T. Murphy, Laura Jenkinson, ..., Gordon S. Lynch, John Silke, Nicholas J. Hoogenraad

Correspondence

a.johnston@latrobe.edu.au (A.J.J.), n.hoogenraad@latrobe.edu.au (N.J.H.)

In Brief

Antibodies against the TWEAK receptor Fn14 prevent tumor-induced cachexia and extend lifespan by inhibiting weight loss and inflammation, although having only moderate effects on tumor growth.

Highlights

- Tumors expressing Fn14 cause cachexia in mice
- Fn14 antibodies extend lifespan by inhibiting tumor-induced cachexia
- Fn14- and TWEAK-deficient mice succumb to cancer cachexia
- Tumor Fn14 signaling, rather than host, is responsible for inducing cachexia

Johnston et al., 2015, Cell *162*, 1365–1378
September 10, 2015
http://dx.doi.org/10.1016/j.cell.2015.08.031

CellPress

Cell

Targeting of Fn14 Prevents Cancer-Induced Cachexia and Prolongs Survival

Amelia J. Johnston,[1,*] Kate T. Murphy,[2] Laura Jenkinson,[1] David Laine,[1] Kerstin Emmrich,[1] Pierre Faou,[1] Ross Weston,[1] Krishnath M. Jayatilleke,[1] Jessie Schloegel,[1] Gert Talbo,[1] Joanne L. Casey,[1] Vita Levina,[1] W. Wei-Lynn Wong,[3] Helen Dillon,[1] Tushar Sahay,[1] Joan Hoogenraad,[1] Holly Anderton,[1,4,5] Cathrine Hall,[4,5] Pascal Schneider,[6] Maria Tanzer,[4,5] Michael Foley,[1] Andrew M. Scott,[7,1] Paul Gregorevic,[8,9] Spring Yingchun Liu,[10] Linda C. Burkly,[11] Gordon S. Lynch,[2] John Silke,[1,4,5] and Nicholas J. Hoogenraad[1,*]

[1]Department of Biochemistry and Genetics, La Trobe Institute for Molecular Science, La Trobe University, Melbourne, VIC 3086, Australia
[2]Basic and Clinical Myology Laboratory, Department of Physiology, The University of Melbourne, Melbourne, VIC 3010, Australia
[3]Institute of Experimental Immunology, University of Zürich, Zürich 8057, Switzerland
[4]The Walter and Eliza Hall Institute, Melbourne, VIC 3052, Australia
[5]Department of Medical Biology, The University of Melbourne, Melbourne, VIC 3050, Australia
[6]Department of Biochemistry, University of Lausanne, Epalinges 1066, Switzerland
[7]Olivia Newton-John Cancer Research Institute, Melbourne, VIC 3084, Australia
[8]Baker IDI Heart and Diabetes Institute, Melbourne, VIC 3004, Australia
[9]Department of Biochemistry and Molecular Biology, Monash University, Clayton, VIC 3800, Australia
[10]Broad Institute, MIT and Harvard, Cambridge, MA 02142, USA
[11]Department of Immunology, Biogen Idec, 14 Cambridge Center, Cambridge, MA 02142, USA
*Correspondence: a.johnston@latrobe.edu.au (A.J.J.), n.hoogenraad@latrobe.edu.au (N.J.H.)
http://dx.doi.org/10.1016/j.cell.2015.08.031

SUMMARY

The cytokine TWEAK and its cognate receptor Fn14 are members of the TNF/TNFR superfamily and are upregulated in tumors. We found that Fn14, when expressed in tumors, causes cachexia and that antibodies against Fn14 dramatically extended lifespan by inhibiting tumor-induced weight loss although having only moderate inhibitory effects on tumor growth. Anti-Fn14 antibodies prevented tumor-induced inflammation and loss of fat and muscle mass. Fn14 signaling in the tumor, rather than host, is responsible for inducing this cachexia because tumors in Fn14- and TWEAK-deficient hosts developed cachexia that was comparable to that of wild-type mice. These results extend the role of Fn14 in wound repair and muscle development to involvement in the etiology of cachexia and indicate that Fn14 antibodies may be a promising approach to treat cachexia, thereby extending lifespan and improving quality of life for cancer patients.

INTRODUCTION

Fn14 (tumor necrosis factor receptor superfamily member 12A; TNFRSF12A) and its ligand TWEAK (TNFSF12) have been shown to play multiple roles in the process of wound repair and can promote angiogenesis, proliferation, migration, apoptosis, and inflammation (Burkly et al., 2011; Campbell et al., 2004; Vince and Silke, 2006; Winkles, 2008). Consistent with such a role, its expression is strongly induced by growth factors in vivo at sites of tissue injury and remodeling (Wiley et al., 2001; Winkles, 2008). Fn14 expression is also increased in solid tumors (Culp et al., 2010; Wiley et al., 2001). Fn14 signaling therefore contributes to carcinogenesis, and targeting this pathway with monoclonal antibodies can inhibit tumor growth (Culp et al., 2010; Winkles, 2008).

Cachexia is a complex disease, best described as a metabolic disorder that includes progressive muscle wasting with or without the loss of fat stores. It frequently presents in the terminal stages of many chronic illnesses, including cancer (Tisdale, 2009), and may be present in 50%–80% of patients with solid tumors (Dewys et al., 1980; Walsh et al., 2000). Although cachexia reduces patient survival and response to chemotherapy and may account for ~25% of all cancer deaths (Warren, 1932), the molecular mechanisms are unknown, and there are no FDA approved drugs to treat it. Attempts to cure cachexia by increasing appetite or nutrition have proven unsuccessful in clinical trials. However, it has been suggested that interventions for cachexia could potentially be developed by targeting inflammatory processes that occur in concert with the wasting and metabolic imbalance that characterize cachexia (Muscaritoli et al., 2010).

Interleukin-1 (IL-1), IL-6, TNF, and interferon-γ are inflammatory cytokines that have been suggested to play a role in cachexia (Argilés et al., 2009; Tisdale, 2009). Glucocorticoids may also contribute to cachexia by upregulating tumor-derived factors such as lipid-mobilizing factor, which activates degradative pathways in adipose tissue leading to the breakdown of fat deposits and disrupted metabolic processes (Islam-Ali and Tisdale, 2001; Russell and Tisdale, 2005). Most recently, it has been shown that activation of the activin type-2 receptor ActRIIb by transforming growth factor β (TGF-β) family ligands drives a cachectic phenotype in mice and the degradation of contractile proteins through the ubiquitin-proteasome pathway. Recombinant decoy ActRIIb inhibited activation of this pathway and

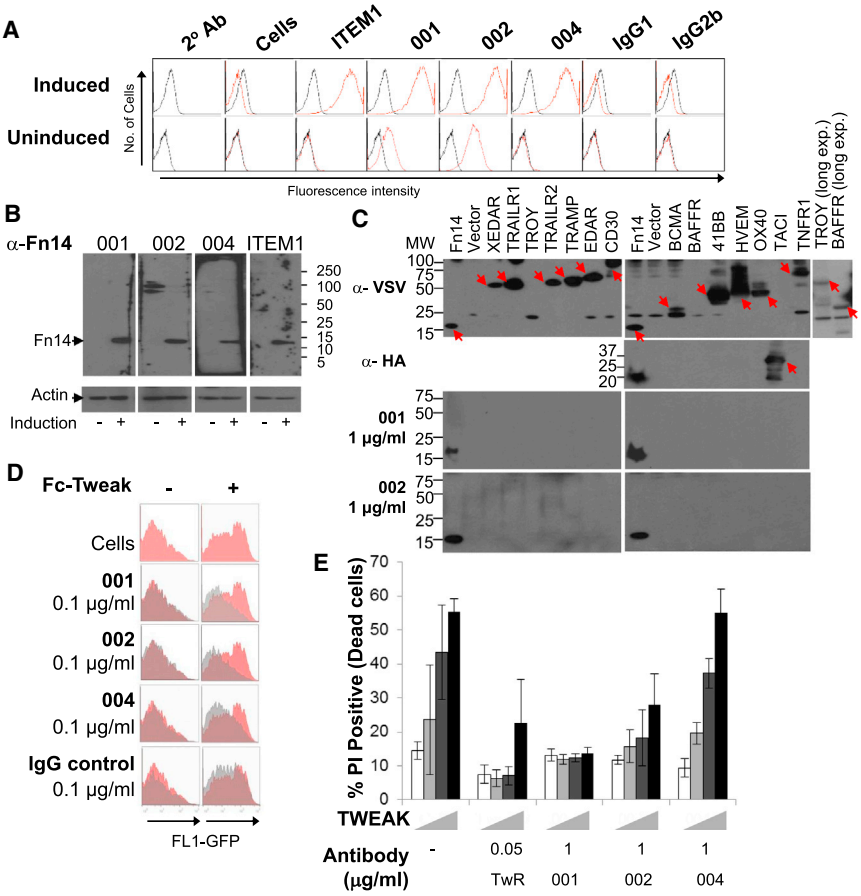

Figure 1. Fn14 Antibodies Antagonize TWEAK/Fn14 Signaling

(A) MEF H-Ras V12 cells expressing inducible hFn14 stained with indicated antibodies. Red: antibody staining; black: secondary antibody alone.

(B) Western blot of lysates from H-Ras V12 MEFs expressing inducible hFn14 ± induction probed with indicated Fn14 antibodies.

(C) Western blot of HEK293T cells transiently transfected with the indicated VSV or HA-tagged TNFSFR probed with indicated antibodies. Arrows indicate the expressed protein. Note 001 blot (right) was reprobed with anti-HA.

(D) GFP fluorescence of HEK293T NF-κB GFP reporter cells stimulated ± 100 ng/ml of Fc-TWEAK for 24 hr (pink), and cells co-incubated with the indicated antibodies (gray).

(E) Kym1 cell-death assay with increasing Fc-TWEAK dose and co-incubated with indicated antibodies for 24 hr, harvested, stained with PI, and percent PI-positive cells assessed determined from flow cytometry.

Data are means ± SEM (n = 3). See also Figure S1.

RESULTS

Monoclonal Antibodies against Fn14

To test the hypothesis that inhibition of Fn14 would limit tumor growth, we generated antagonist monoclonal antibodies against Fn14 by inoculating wild-type mice with recombinant human Fn14-Fc and generated hybridomas as previously described (Galfrè and Milstein, 1981). Three monoclonal antibodies, 001, 002, and 004, were positive against a mouse embryonic fibroblast (MEF) cell line stably expressing inducible human Fn14 (hFn14; Figure 1A), as was a commercially available control anti-human Fn14, ITEM1 (Nakayama et al., 2003). ITEM1 and our three antibodies detected hFn14 specifically by western blot (Figure 1B). Human and mouse Fn14 are 92% identical in the extracellular domain, and two of the antibodies, 001 and 002, reacted against the uninduced MEF cell lines that express endogenous murine Fn14 (Figure 1A).

Because members of the TNF receptor superfamily (TNFRSF) share homology in their extra-cellular domains, these proteins are most likely to cross-react with Fn14 antibodies. However, several are only expressed in specific hematopoietic lineages, making it difficult to rule out cross-reactivity by screening cell lines. Therefore, VSV- or HA-tagged TNFRSF members were overexpressed in HEK293T cells and reacted with either a VSV, HA, 001, or 002 antibody. All TNFRSF receptors were expressed and detected by VSV or HA antibodies; however, only Fn14 was detected by 001 and 002 (Figure 1C).

TWEAK activates both canonical and non-canonical NF-κB signaling pathways (Salzmann et al., 2013; Varfolomeev et al., 2007, 2012; Vince et al., 2008). To address whether the Fn14 antibodies activated or blocked Fn14-dependent signaling, we

significantly increased survival and muscle mass of mice bearing cachexia-inducing tumors (Zhou et al., 2010). Unfortunately, however, decoy ActRIIb in clinical trials resulted in treatment-related bleeding issues in healthy adults and boys with Duchenne muscular dystrophy and were therefore stopped and have not been pursued for cachexia treatment.

Because of the demonstrated involvement of Fn14 signaling in tumor progression, we began our studies with the hypothesis that an antagonistic monoclonal antibody targeting Fn14 would inhibit tumor growth (Vince and Silke, 2006; Winkles, 2008). We developed and characterized three antagonist monoclonal antibodies against Fn14. Two of these antibodies showed variable ability to block tumor growth but were strikingly effective at preventing tumor-induced weight loss. We demonstrated that the tumor-induced loss of lean and fat mass is consistent with the development of cachexia. In addition, our Fn14 antibodies were able to prevent and reverse tumor-induced cachexia in different tumor models. We also demonstrated that the role of Fn14 in cachexia is independent of both host- and tumor-derived TWEAK. We further showed that although reported to be upregulated during atrophy, muscle-localized Fn14 is not actively involved in the loss of muscle mass, supporting the idea of an alternative role such as repair/regeneration. Our results support the hypothesis that inhibiting Fn14 signaling has therapeutic potential for cancer-induced cachexia.

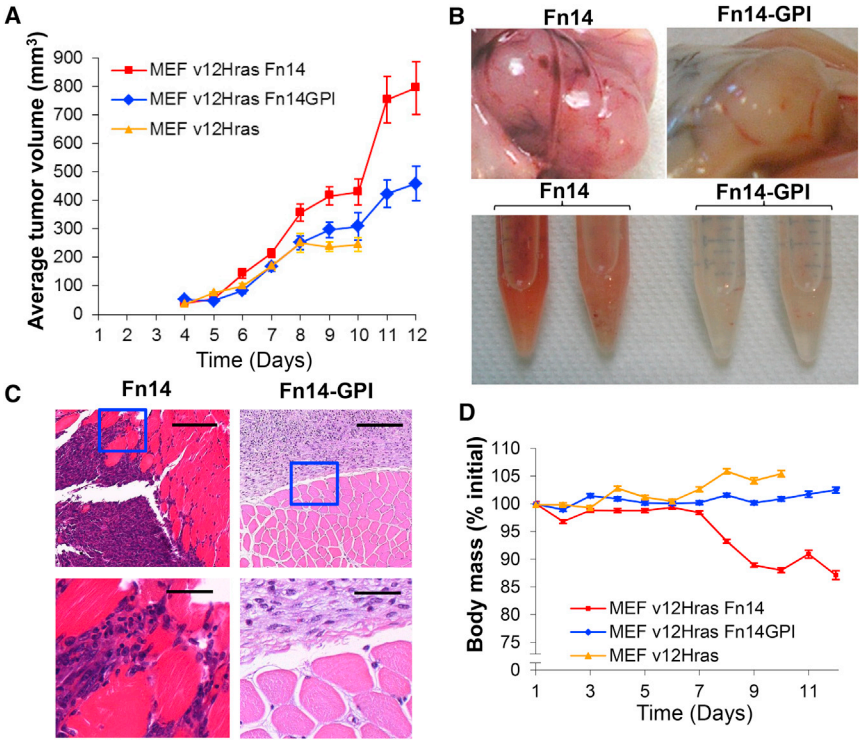

Figure 2. Ectopic Fn14 Expression in Tumors Causes Loss of Body Weight

(A) Female C57BL/6 mice injected with 5 × 10^6 tumor cells (day 1). Mean tumor volume ± SEM of three independent experiments (Fn14, n = 26; Fn14-GPI, n = 20; H-Ras, n = 6).

(B) Representative images of in situ tumors from Fn14-expressing tumors (left) or Fn14-GPI-expressing tumors (right). Bottom image, disaggregated individual tumors from Fn14 (left) and Fn14-GPI (right).

(C) Fixed tumor sections stained with H&E. Left: Fn14-expressing tumor, and right: Fn14-GPI-expressing tumor taken on day 11. Images are 10× (upper, scale bar 160 μm) and 40× magnification (lower, scale bar 40 μm). Blue box represents area shown in 40× images.

(D) Body weight from mice in (A) standardized against starting weight. Data are means ± SEM.

used a HEK293T cell line that expresses endogenous hFn14, stably transduced with a lentiviral NF-κB reporter vector (Vince et al., 2008; Figure 1D). The antibodies were unable to stimulate NF-κB, demonstrating that, in this assay, they are not Fn14 agonists (left column, Figure 1D). They did however block TWEAK/hFn14-induced NF-κB (right column, Figure 1D). To functionally assess the ability of our antibodies to inhibit TWEAK/hFn14 signaling, we used Kym1 cells that are sensitive to cell death induced by TWEAK (Schneider et al., 1999; Vince et al., 2008). We co-incubated Kym1 cells ± TWEAK (at 5, 50, or 200 ng/ml) and monoclonal antibodies at a concentration of 1 μg/ml for 24 hr. Adherent and floating cells were harvested and stained with propidium iodide (PI), and the percentage of dead, PI-positive cells was determined by flow cytometry. Antibodies 001 and 002, but not 004, inhibited TWEAK-induced death of Kym1 cells (Figure 1E).

Consistent with results from the other assays, 001 and 002 bound both recombinant human and mouse Fn14 extracellular domains, whereas ITEM1 bound better to hFn14 than to mouse (Figure S1A). To define the epitope, we generated two "sub-domains" of the extracellular domain of Fn14 as peptides (Brown et al., 2006) and assessed antibody binding by quantitative ELISA. All antibodies bound efficiently and specifically to sub-domain 2 but not to sub-domain 1 (Figures S1B and S1C). These results demonstrate that IgG2b 001 and IgG1 002 antibodies bind specifically to an extracellular epitope present on both human and mouse Fn14 receptor.

Fn14-Expressing Tumors Cause Severe Weight Loss in Mice

To test our hypothesis that an Fn14 antibody could inhibit tumor growth, we generated an Fn14-expressing tumor cell line and equivalent control cell lines to generate tumors in wild-type mice. MEFs derived from C57BL/6 embryos and transformed with an H-Ras V12 oncogene were infected with an hFn14-expressing lentivirus. As a control, we infected the same parental cell line with a lentivirus expressing only the extracellular domain of hFn14 fused to a GPI anchor. Both hFn14 and control cell lines formed tumors when injected into syngeneic C57BL/6 mice and initially grew at similar rates (Figure 2A). Post-mortem analysis of these mice revealed increased vasculature (Figure 2B) and tumor-invasive capacity (Figure 2C) in the hFn14-expressing tumors when compared with controls. Surprisingly, 8 days post-inoculation, mice bearing hFn14-expressing tumors, but not the control tumors, suffered rapid weight loss, and their overall health deteriorated quickly (Figure 2D). It was apparent the mice bearing Fn14 tumors were suffering from cachexia.

Fn14 Antibodies Block Fn14-Induced Cachexia in Mice

We next assessed the effect of anti-Fn14 therapy using the monoclonal antibody 001 against the weight loss seen in the mice bearing Fn14-expressing tumors. Mice were inoculated with MEF tumor cells expressing Fn14 or not and just prior to expected weight loss (day 6) were treated with 001 or an IgG2b isotype control. These hFn14-expressing tumors caused a rapid loss of body mass, and a single treatment with anti-Fn14, but not the control antibody, substantially prevented this loss (Figures 3A and S2A), even though tumor mass and volume were not significantly different between groups (Figure S2B). Fn14 tumors caused a decrease in mass of the tibialis anterior (TA) and plantaris muscles and a trend for lower muscle mass of extensor digitorum longus (EDL), soleus, gastrocnemius, and quadriceps (Figure 3B). There was no significant change in heart mass in Fn14 tumor-bearing mice (Figure 3C) but a significant decrease in subscapular fat mass (Figure 3D). The loss of muscle and fat mass in hFn14-expressing tumor mice was reduced by a single injection of anti-human Fn14 antibody (Figures 3B–3D).

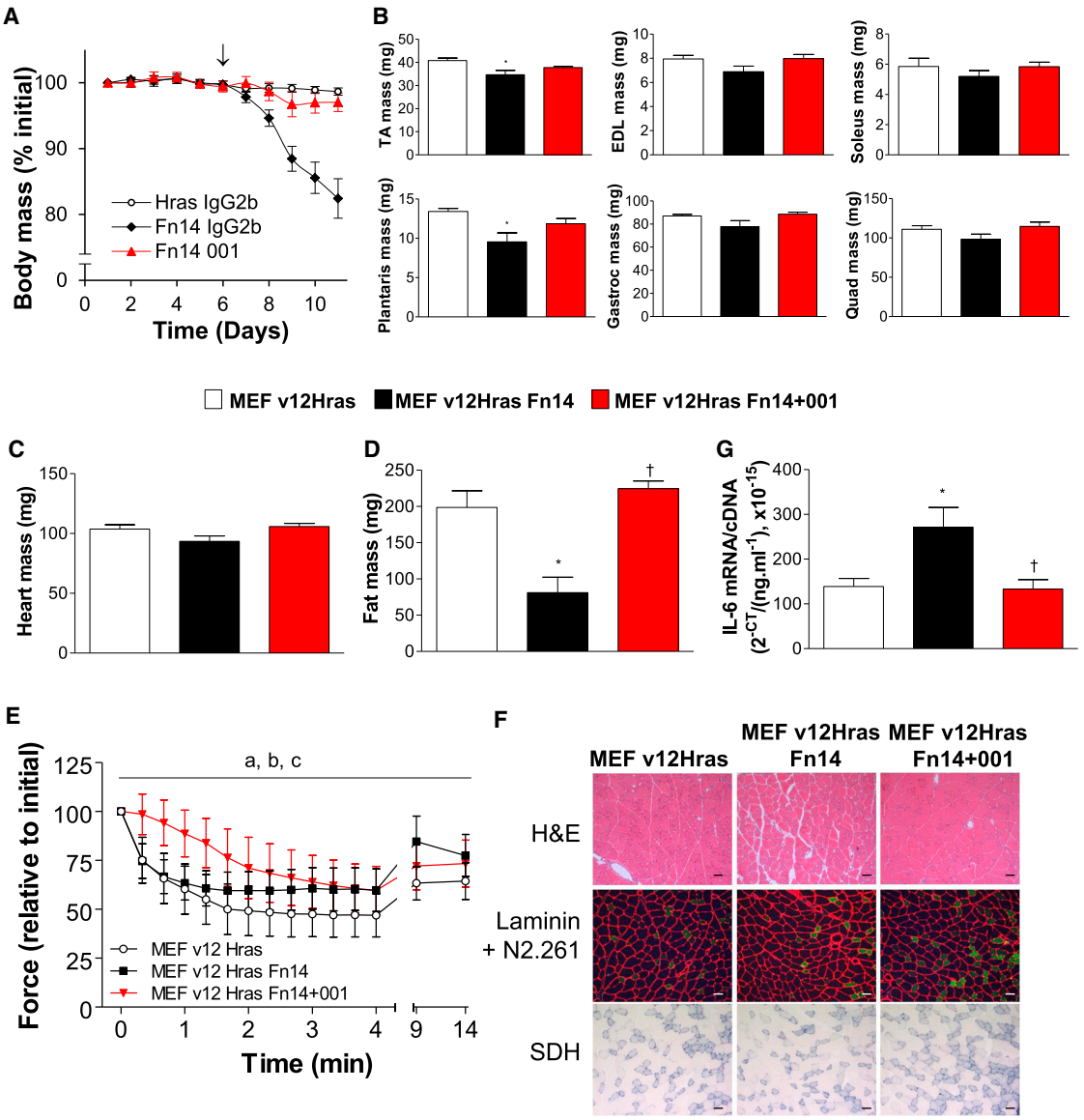

Figure 3. Anti-Fn14 Prevents Cachexia Caused by Fn14 Tumors

Female C57BL/6 mice inoculated with MEFs transduced with Fn14 (H-Ras V12 Fn14) or the parental MEF line (H-Ras V12) on day 1. Mice were treated with IgG2b control (H-Ras V12, H-Ras V12 Fn14, n = 8/group) or 001 (H-Ras V12 Fn14+001, n = 8) on day 6.

(A) Group body mass standardized against starting weight ± SEM. Antibody treatment (↓; 5 mg/kg).

(B) Day 11, muscles were excised and weighed. TA: tibialis anterior, EDL: extensor digitorum longus, Gastroc: gastrocnemius, Quad: quadriceps.

(C) Heart and (D) subscapular fat were excised and weighed. Data are means ± SEM (n = 8).

(E) Tetanic force production (expressed relative to initial maximum force) during and after 4 min of fatiguing intermittent stimulation in TA muscles in situ. Data are means ± SEM (n = 8).

(F) Frozen TA muscle sections stained with H&E and reacted for anti-laminin (red), anti-myosin IIa (N2.261, green), and SDH activity (blue). Scale bar represents 100 μm.

(G) Quantitation of IL-6 mRNA in TA muscles.

*p < 0.05 versus MEF v12 Hras; †p < 0.05 versus MEF v12 Hras Fn14. [a]p < 0.05 main effect MEF v12 Hras versus MEF v12 Hras Fn14, [b]p < 0.05 main effect MEF v12 Hras versus MEF v12 Hras Fn14+001, [c]p < 0.05 main effect MEF v12 Hras Fn14 versus MEF v12 Hras Fn14+001. Data are means ± SEM (n = 8).

See also Figure S2.

In addition, the contractile properties of muscles in live mice were assessed on day 11, but there were no significant differences between groups in grip strength (data not shown), and in anesthetized mice there were no differences in peak twitch force (data not shown), peak tetanic force, and specific (normalized) force of TA muscles in situ (Figure S2C). However, tetanic force over a range of stimulation frequencies (10–300 Hz) was lower in TA muscles from mice with hFn14 tumors than from mice bearing control

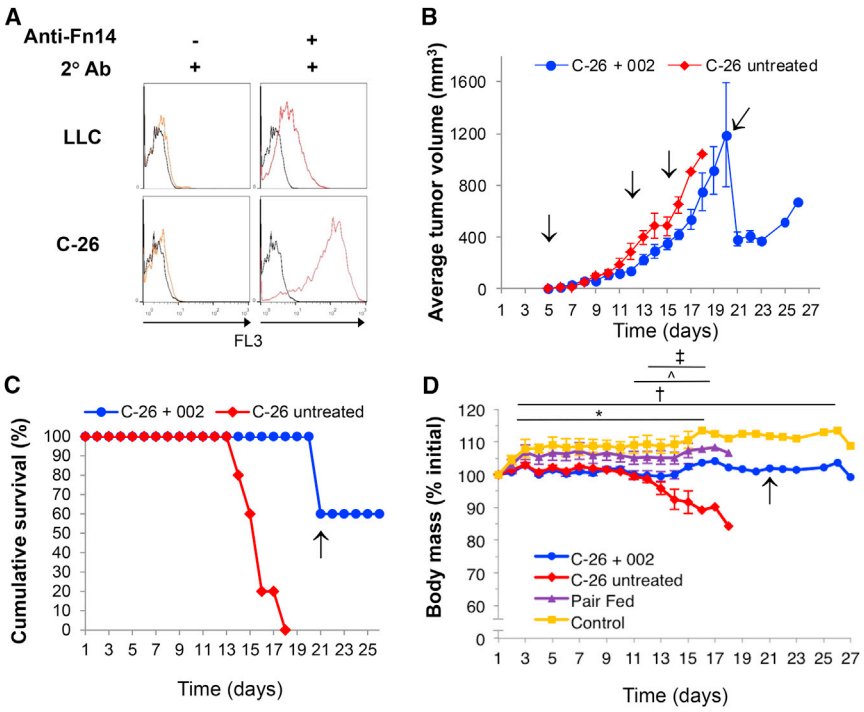

Figure 4. Fn14 Antibodies Prevent Tumor-Induced Weight Loss

(A) Flow cytometric analysis of mouse tumor cell lines LLC and C-26 adapted to low serum (0.5% FCS) and stained with anti-Fn14 (ITEM1). Black trace: unstained cells, orange trace: secondary stain only, red trace: anti-Fn14.

(B) Average tumor volume for CD2F1 male mice inoculated with 1 × 10^6 cells (s.c., day 1). Data are means ± SEM. Antibody treatment (↓); 10 mg/kg. *$p < 0.05$ versus C-26.

(C) A Kaplan-Meier survival curve. $p < 0.01$ log-rank (Mantel-Cox) test.

(D) Group average mouse weight standardized to starting weight ± SEM. *$p < 0.05$ control versus C-26; †$p < 0.05$ control versus C-26+002; ˆ$p < 0.05$ pair-fed versus C-26; ‡$p < 0.05$ C-26 versus C-26+002.

Drop in average tumor volume of treated animals at day 21 in (B) coincides with culling of two mice due to ethical considerations (also noted by ↑ in C and D).

tumors, and this reduction in force was prevented by treatment with anti-Fn14 (Figure S2C, top panel). Anti-Fn14 also increased relative force production during and after a 4 min intermittent fatiguing stimulation protocol, indicating reduced muscle fatigability following anti-human Fn14 treatment (Figure 3E).

TA muscle sections were stained with hematoxylin and eosin (H&E), anti-laminin, and anti-myosin IIa to examine the effect of Fn14 tumor expression on muscle fiber architecture and cross-sectional area (Figure 3F). Tumors expressing hFn14 caused decreased muscle fiber cross-sectional area (Figure S2D), which was due to decreases in size of both type IIa and type IIx/b fibers (Figure S2E). A single injection of anti-Fn14 prevented the decrease in muscle fiber size (Figures 3F and S2D). Despite improvements in muscle fatigability, anti-Fn14 did not cause a shift in fiber-type proportions (Figures 3F and S2E) or muscle fiber oxidative capacity as assessed by succinate dehydrogenase (SDH) reaction intensity (Figures 3F and S2E). Assessment of mRNA levels of IL-6, an inflammatory marker of cachexia in TA muscle, also revealed that hFn14 tumors caused a significant increase in IL-6 expression in TA muscles compared to control tumors, and anti-Fn14 treatment blocked this increase (Figure 3G).

Fn14 Antibodies Increase Survival of Colon-26 Tumor-Bearing Mice

Given that tumor-expressed Fn14 had not been previously reported as a mediator of cachexia, it was important to assess whether this finding was more widely applicable. We therefore chose well-published mouse models of cachexia to further validate our findings. We assessed the level of Fn14 expression on two such tumor cell lines, Lewis lung carcinoma (LLC) and colon-26 (C-26), and demonstrated that they express low and high Fn14 levels, respectively (Figure 4A).

We chose to establish and utilize the C-26 tumor model to test the efficacy of anti-Fn14 given that the cell line expressed high levels of Fn14, and this model generally displays more marked cachexia. Groups of five immunocompetent CD2F1 mice were inoculated with C-26 tumor cells, then treated or not with antibody 002 on days 5, 12, 15, and 20 post-inoculation. We chose monoclonal antibody 002 for this model given that it reacted slightly stronger than 001 to mouse Fn14 (Figure 1A). Antibody 002 is a different isotype than 001 and also has a subtly different Fn14 binding profile and ability to block Fn14 signaling compared to antibody 001. The tumors grew well, and although they displayed some inter-individual heterogeneity, growth was slightly slower in the treated compared to the untreated mice (Figure 4B). The survival of the treated mice was also extended dramatically (Figure 4C), and although the tumors in untreated and treated animals were comparable in size over the 18 days post-inoculation, untreated mice lost weight rapidly from day 11 onward, whereas treated mice maintained weight and condition during this period (Figure 4D). Maintenance of weight in a pair-fed control group showed that the loss in body mass in the untreated C-26 tumor mice was not due to differences in food intake (Figure 4D).

Fn14 Antibodies Block C-26 Tumor-Induced Cachexia

To more extensively characterize the weight loss and effect of anti-Fn14 treatment on C-26 tumor-bearing mice, we treated 10 mice with either anti-Fn14 002 or an isotype control IgG dosed on days 8, 12, and 16 post tumor inoculation and sacrificed them at day 22. The experiments presented in Figures 5 and 6 were performed in different labs with different sources of C-26 tumor cell lines than those presented in Figure 4, and as observed before, untreated C-26 tumor mice began to lose weight around 11 days post tumor inoculation. Although there was a slightly slower decline in weight using this alternative source of C-26 cells, anti-Fn14-treated mice again retained

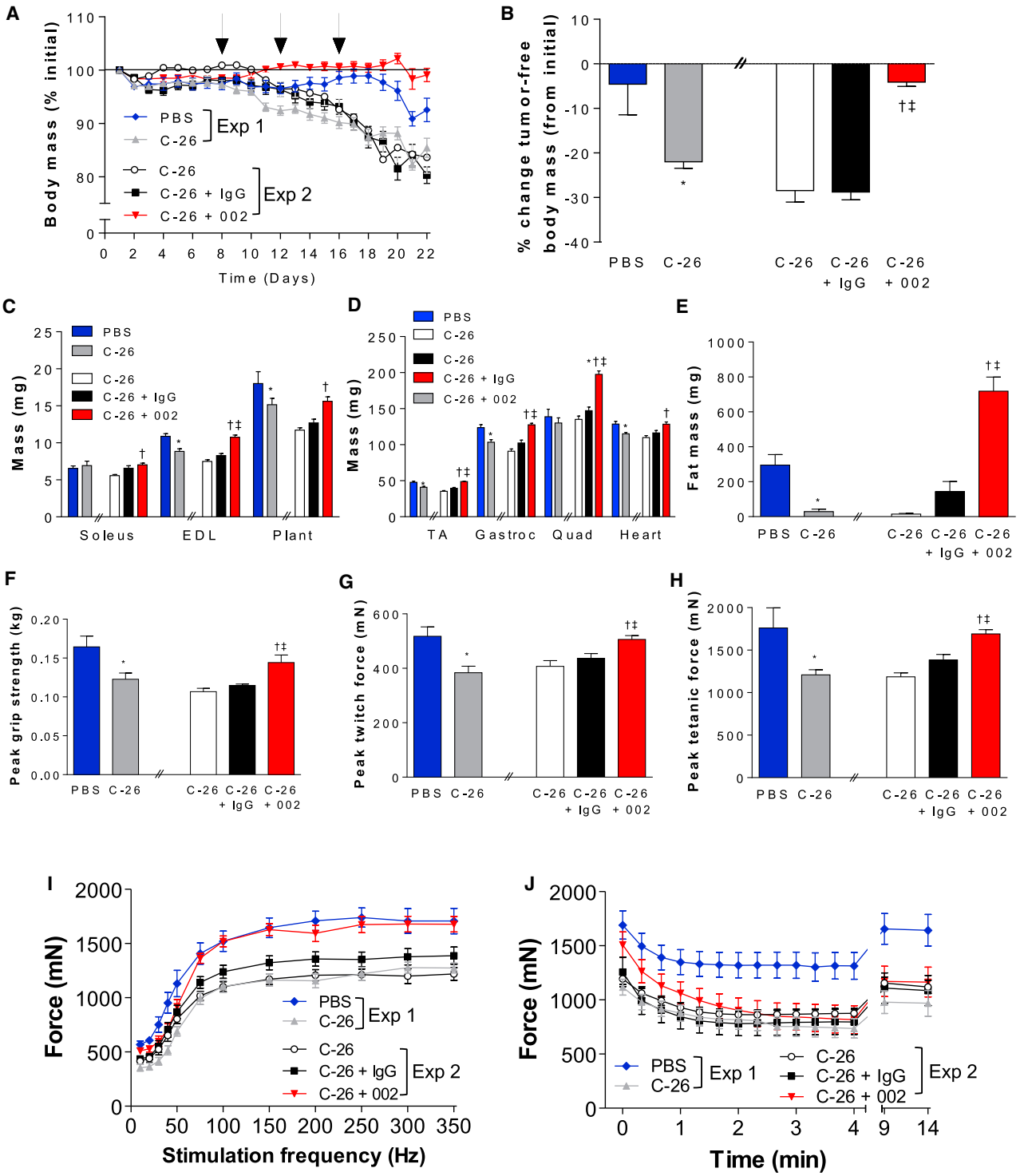

Figure 5. Fn14 Inhibition Attenuates Muscle Wasting and Weakness in C-26 Tumor-Bearing Mice

(A) Group average body weight standardized to starting weight ± SEM of CD2F1 mice inoculated with PBS or 0.5 × 10^6 C-26 cells s.c. (day 1). Antibody injections (↓; 10 mg/kg). Relative body mass of C-26 from experiment 1 (gray, n = 23) significantly lower than PBS (blue, n = 14) from day 14 ($p < 0.05$). Body mass of C-26 from experiment 2 (white, n = 10) significantly lower than pair-fed 002-treated C-26 (red, n = 10) from day 16 ($p < 0.05$). Pair-fed IgG-treated C-26 (black, n = 10) body mass significantly lower than 002-treated C-26 from day 13 ($p < 0.05$).

(B) Day 22, tumors excised and weighed, and percent change in tumor-free body mass compared to pre-inoculation weight calculated. Data represent means ± SEM. *$p < 0.05$ versus PBS; †$p < 0.05$ versus C-26 from experiment 2; ‡$p < 0.05$ versus pair-fed IgG-treated C-26.

(legend continued on next page)

body weight (Figure 5A, Exp 1). We also assessed untreated C-26 tumor-bearing mice and a non-tumor group that were injected with PBS in place of C-26 cells and pair-fed against the C-26 group (blue and gray lines, respectively), and the data indicate reproducibility and that weight loss is unlikely due to food intake (Exp 2). Tumors in antibody-treated mice grew slower than in control mice, but weight loss was well advanced by day 17 when tumor size differences were negligible, indicating that the anti-tumor effect of the antibody was not the reason for the reduction in cachexia (Figures 5A and S3A). The preservation of weight in the anti-Fn14-treated mice was more apparent when the weights of the mice without tumors were measured (Figure 5B). Furthermore, the mass of several muscles in anti-Fn14-treated mice was significantly spared compared to control IgG-treated mice (Figures 5C and 5D). Heart and fat mass were also spared in anti-Fn14-treated mice (Figures 5D and 5E). Consistent with the preservation of muscle mass, peak grip strength in living mice at day 21 was increased in anti-Fn14-treated mice compared to control IgG-treated mice (Figure 5F). Peak twitch force (Figure 5G), peak tetanic force (Figure 5H), and tetanic force over a range of stimulation frequencies (Figure 5I) of TA muscles assessed in situ were also higher in anti-Fn14-treated animals compared to control-treated mice. After determining peak tetanic force, muscles were subjected to a 4 min intermittent stimulation protocol to induce muscle fatigue. Again, TA muscles of anti-Fn14-treated mice produced higher forces throughout most of the fatiguing stimulation protocol than control treated mice (Figure 5J).

These results demonstrated that the cachexia seen in C-26 tumor-bearing mice was caused by Fn14 and that those mice treated with anti-Fn14 antibody were not succumbing to cachexia. To investigate this at the cellular level, TA muscle sections were stained with H&E, revealing a larger fiber size in anti-Fn14-treated mice compared with the control treated mice (Figure 6A). Sections stained with anti-laminin confirmed the preservation of fiber size in anti-Fn14-treated mice (Figures 6B and S3B), and co-staining with a myosin IIa-specific antibody (N2.261) to identify type IIa and type IIx/b fibers revealed that the cross-sectional area of both fast, oxidative type IIa fibers and fast, glycolytic type IIx/b fibers was increased by anti-Fn14 treatment (Figures 6C and 6D). The proportion of type IIa and type IIx/b fibers was similar between treated and untreated groups (Figure 6D), as was muscle fiber oxidative capacity as assessed by SDH (Figures 6C and S3C). These results show that protection of muscle mass and strength with anti-Fn14 treatment was due to the protection of individual muscle fibers and not a shift in muscle fiber-type composition.

Muscle atrophy has been shown to occur through activation of the ubiquitin proteasome and inhibition of the Akt/p70S6K pathway in muscle (Dogra et al., 2007). We therefore investigated the effect of anti-Fn14 treatment on the mRNA expression of the ubiquitin ligases MuRF-1 and atrogin-1 in the TA of these cachectic mice. Consistent with the increase in muscle mass and fiber size in anti-Fn14-treated mice, MuRF-1 and atrogin-1 mRNA expression was reduced in the TA muscles of anti-Fn14-treated tumor-bearing mice compared with untreated and IgG-treated mice (Figure 6E). In addition to loss of muscle, mRNA expression of the inflammatory cytokines IL-6 and TNF were significantly higher in TA muscles from C-26 control and control IgG-treated mice compared to anti-Fn14-treated mice, indicating that anti-Fn14 protects mice from muscle loss and also reduces the cachectic inflammatory phenotype (Figure 6F).

Not All Fn14 Antibodies Are Anti-cachectic

Given the complete blockade of cachexia onset and progression with the two antibodies we had tested, we next investigated whether any Fn14 antibody would be efficacious against the symptoms of cachexia. We assessed a third antagonistic antibody, 004, along with a commercially available antibody that has been reported to be a weak agonist, ITEM1. 004 is specific to human Fn14 and unlike either 001 or 002 did not cross-react with murine Fn14. Given that the MEF Fn14 tumor model expressed human Fn14, this was an ideal model to test for efficacy of this antibody. ITEM1, unlike 001, 002, or 004, did not antagonize or agonize TWEAK/Fn14 signaling in the NF-κB reporter assay (Figures 1D and S4A). Human Fn14-expressing MEF tumors were established in mice, and a single dose of antibody was administered at day 7, just prior to noticeable weight loss (Figures S4B–S4D), or day 8, the first day of weight loss (Figures S4E and S4F), to randomized groups of mice. Consistent with the preceding experiments, 001 and 002 prevented weight loss induced by Fn14 tumors (Figures S4B, S4D, and S4E) and improved survival (Figures S4C and S4F). However, 004 and ITEM1 were unable to prevent Fn14 tumor-induced weight loss or improve survival. These results suggest that neither the ability

(C–E) Day 22, selected tissues were excised and weighed. (C) EDL: extensor digitorum longus, Plant: plantaris. (D) TA: tibialis anterior, Gastroc: gastrocnemius, Quad: quadriceps. (E) Epididymal fat. Data are means ± SEM. *$p < 0.05$ versus PBS; †$p < 0.05$ versus C-26; ‡$p < 0.05$ versus pair-fed IgG-treated C-26.

(F) Day 21, whole-body strength was assessed using a grip-strength meter. Data are means ± SEM. *$p < 0.05$ versus PBS; †$p < 0.05$ versus C-26 from experiment 2; ‡$p < 0.05$ versus pair-fed IgG-treated C-26.

(G and H) Day 22, (G) peak twitch force and (H) peak tetanic force of TA muscle were assessed in situ. Data are means ± SEM. *$p < 0.05$ versus PBS; †$p < 0.05$ versus C-26 from experiment 2; ‡$p < 0.05$ versus pair-fed IgG-treated C-26.

(I) Day 22, tetanic force production at stimulation frequencies of 10–350 Hz assessed in TA muscles in situ. Data are means ± SEM. Force from C-26 from experiment 1 (gray, n = 9) significantly lower than PBS (blue, n = 7) from 30 Hz ($p < 0.05$). Force from C-26 experiment 2 (white, n = 9) significantly lower than pair-fed 002-treated C-26 (red, n = 10) from 75 Hz ($p < 0.05$). Force from pair-fed IgG-treated C-26 (black, n = 9) significantly lower than 002-treated C-26 from 100–200 Hz ($p < 0.05$).

(J) Tetanic force production during and following 4 min fatiguing intermittent stimulation assessed in TA muscles in situ. Data are means ± SEM. Force lower in C-26 from experiment 1 (gray, n = 8) compared to PBS (blue, n = 7, $p < 0.001$ group main effect). Force lower in C-26 from experiment 2 (white, n = 8) and pair-fed IgG-treated C-26 (black, n = 9) compared to pair-fed 002-treated C-26 (red, n = 10, $p < 0.001$ group main effect).

Exp 1 and Exp 2: experiments 1 and 2, respectively. In graphs in (B)–(F), double forward slash (//) denotes data obtained in two separate experiments. See also Figure S3.

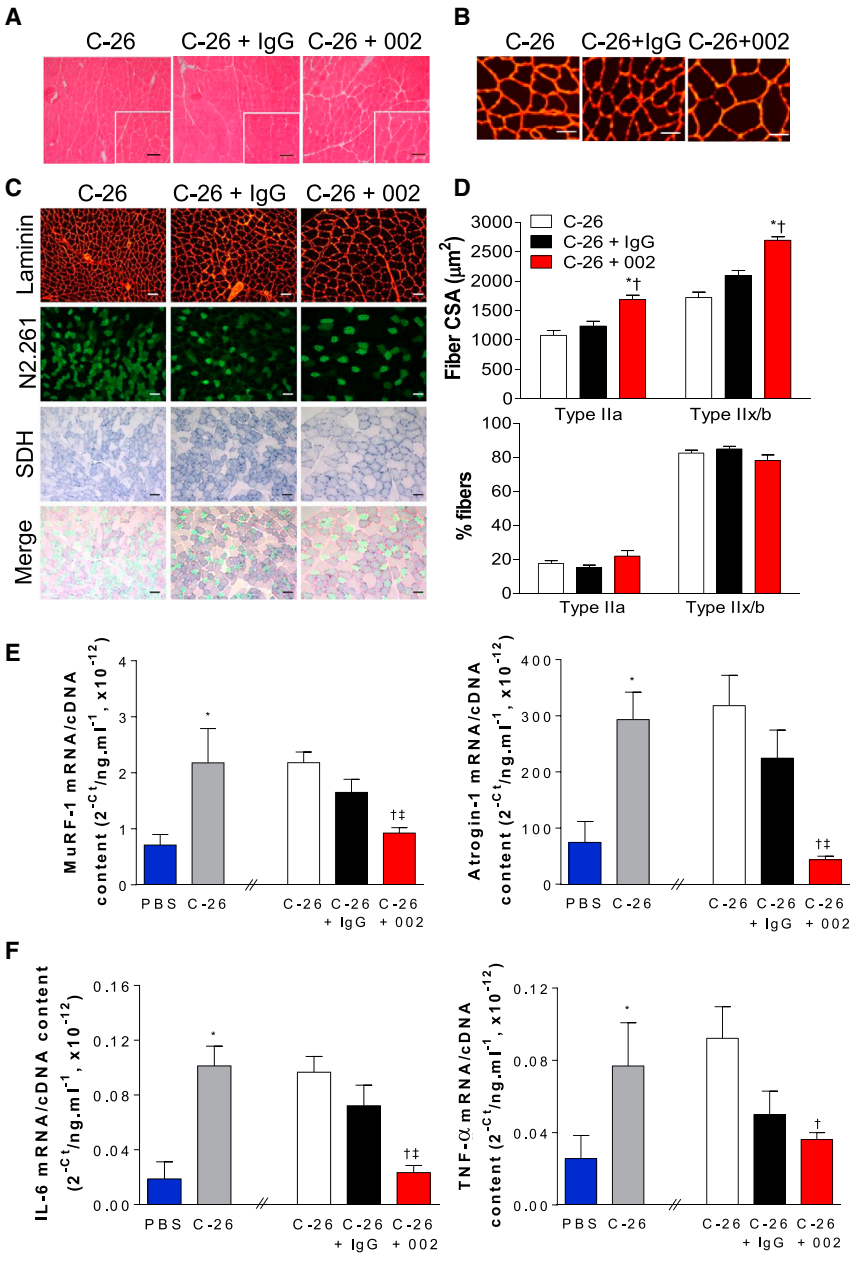

Figure 6. Fn14 Inhibition Induces Muscle Fiber Hypertrophy

CD2F1 mice were inoculated with 0.5 × 10^6 C-26 cells s.c. (day 1) and treated with indicated antibody (10 mg/kg; days 8, 12, and 16).

(A) Day 22, TA muscles excised and frozen for histological analysis. Representative images of muscle cross-sections stained with H&E and higher magnification inset are shown. Scale bar represents 100 μm.

(B) Muscle sections stained with anti-laminin (scale bar represents 100 μm). See also Figure S3B for quantification of muscle fiber cross-sectional area (CSA).

(C) Representative images of muscle sections and reacted for anti-laminin (red), anti-myosin IIa (N2.261, green, type IIa fibers), and SDH (blue, fiber oxidative capacity). Scale bar represents 100 μm.

(D) Laminin and N2.261 staining from (C) was used to quantify CSA (top) and relative proportion (bottom) of type IIa and type IIx/b fibers. Data are means ± SEM. *p < 0.05 versus C-26; †p < 0.05 versus pair-fed IgG-treated C-26 (n = 8).

(E) MuRF-1 and atrogin-1 mRNA in TA muscles were quantitated. *p < 0.05 versus untreated PBS; †p < 0.05 versus untreated C-26 from experiment 2; ‡p < 0.05 versus pair-fed IgG-treated C-26 (n = 8–9). Data are means ± SEM.

(F) Fn14 inhibition reduced expression of the pro-inflammatory cytokines IL-6 and TNF, and mRNA in TA muscles was quantitated. Mean ± SEM. *p < 0.05 versus PBS; †p < 0.05 versus C-26; ‡p < 0.05 versus pair-fed IgG-treated C-26 (n = 8–9).

Double forward slash (//) denotes data obtained in two separate experiments. See also Figure S3.

to bind human Fn14 nor antagonistic properties of an antibody to human Fn14 are sufficient to predict its ability to inhibit cachexia.

Host TWEAK and Fn14 Do Not Cause Cachexia

TWEAK/Fn14 signaling directly in muscle tissue has been reported to play a role not only in muscle development but also in muscle atrophy (Tajrishi et al., 2014). It was therefore important to determine whether Fn14 or TWEAK from the host tissue could be promoting the Fn14-dependent muscle loss seen in our MEF Fn14 cachexia model. In separate experiments, we established Fn14 tumors in *Fn14*$^{-/-}$ or *Tweak*$^{-/-}$ mice and compared these to tumors in wild-type mice. Mice were inoculated with Fn14 or Fn14-GPI tumor cells on day 1, and body weight and tumor size were monitored (Figure 7). Body, tumor, muscle, and epididymal fat weight were assessed (Figures 7A–7C and S5), and there were no differences in the onset, severity, or timing of cachexia in either strain of knockout mice, suggesting that the signal for cachexia does not originate in host tissues but in the Fn14-expressing tumor cells.

Although these experiments were able to demonstrate that host TWEAK was not a player in cachexia, it was crucial to determine whether the tumor itself was a source of TWEAK involved in cachexia onset. We used the monoclonal TWEAK antibody MTW-1 for this purpose as it has been shown to effectively block the action of TWEAK in mice at reducing collagen-induced arthritis (Kamata et al., 2006). We confirmed in vitro that MTW-1, but not an isotype control antibody (Rat IgG1), blocked TWEAK-induced NF-κB (Figure 7D). Wild-type mice bearing MEF Fn14 tumors were treated with MTW-1 or isotype control on day 7, and body weight was monitored over time. In contrast to the anti-Fn14 antibody treatment, MTW-1 (anti-TWEAK) had no effect on the rapid induction of cachexia by the Fn14 tumor (Figure 7E). Together, these results suggest that neither tumoral nor humoral sources

of TWEAK drive cachexia in this model and that the Fn14/TWEAK signaling pathway in muscle is not responsible for muscle atrophy.

Further Assessment of the Role of Muscle Fn14 in Atrophy

Given that the TWEAK/Fn14 pathway in muscle has been previously implicated in the induction of muscle atrophy pathways, yet our studies in knockout mice suggested no involvement, we next used a specific model whereby atrophy is induced in muscle by the expression of activin A, a soluble molecule well known for its involvement in binding the ActRIIb receptor on muscle cells and activating muscle atrophy pathways. We chose this model because recently, using next-gen sequencing, we found that muscle wasting induced by local transduction of mouse limb muscles with a recombinant adeno-associated virus-based vector expressing activin A (AAV:ActA) was associated with upregulation of Fn14 transcription. Abundance of Fn14 protein was increased approximately 10-fold in muscles administered the activin-expressing vector, compared with contralateral limb controls (Chen et al., 2014). Because local overexpression of activin A was proven to induce Fn14 expression in this muscle atrophy model, we asked whether induction of Fn14 was responsible for causing muscle wasting in activin A-overexpressing muscle or as a downstream consequence of atrophy pathway activation. To test this, we transduced the right TA muscle of C57BL/6 mice with an AAV vector expressing activin A and a control AAV vector in the left muscle. Mice were treated with Fn14 antibodies 001 or 002 or an IgG control antibody 4 days after administration of AAV vectors, for a total of six injections prior to assessment at the experimental endpoint 4 weeks later. Increased local expression of activin A caused muscle wasting as expected (Figures 7F and 7G); however, neither 001 nor 002 blocked activin A-induced muscle loss, indicating that although Fn14 is upregulated in muscle during activin A-induced muscle wasting, it does not cause loss of muscle mass.

Translation to Human Cancer

Given the dramatic pro-cachectic effects of Fn14-expressing tumors in mice, we were interested to see whether there were data that might indicate whether the same scenario pertains to human cancers. We examined the mRNA expression for a range of cancers in the GDAC (Genome Data Analysis Centre) Firehose at the Broad Institute. As with most databases, the presence of weight loss is unfortunately not annotated. However, for cancers where sufficient sample sizes exist, we were able to demonstrate a positive correlation for the expression of Fn14 with pro-inflammatory cytokines in human cancers (Figures S6 and S7). In breast, head and neck, lung, colorectal, and stomach cancer, IL-1α, IL-1β, IL-6, IL-8, and TNF (Figures S6 and S7) all correlate positively with Fn14 expression.

DISCUSSION

We developed antibodies to specifically block Fn14 signaling in order to test the hypothesis that they would reduce tumor growth and development. Our antibodies were specific and selected on the basis that they inhibited TWEAK/Fn14-induced NF-κB signaling and cell death. We initiated studies in vivo on the basis that these antagonistic antibodies might impede tumor growth. Our antibodies, however, have incomplete and tumor-specific effects on tumor growth.

When we expressed Fn14 on tumors (MEF Fn14 model), it surprisingly induced severe weight loss and overall decline in health. Tumors can cause anorexia or suppress appetite (Macciò et al., 2012), but loss of weight in these mice was not due to a tumor effect on feeding because pair-fed controls retained body mass. Cachexia occurs in the presence of other illness, and cancer is one such example. The defining hallmark of cachexia is loss of lean muscle mass and, in some cases, loss of fat. The poor understanding of the signaling pathways that cause cachexia has meant that current cachexia therapies generally target the disease symptoms rather than the cause. For example, ghrelin, a peptide hormone originally isolated from the stomach that stimulates appetite, has been used in cachectic patients to combat loss of body mass (Macciò et al., 2012). However, this is ultimately ineffective because it does not address the cause of the disease.

We therefore investigated the possibility that signaling via Fn14 might contribute to cachexia. In our experiments, untreated and control-treated tumor-bearing mice lost significant muscle mass from all of the major skeletal muscles, and this loss was prevented by treatment with anti-Fn14. Furthermore, muscle function, along with fat stores, were also retained in the antibody-treated mice, and a decrease in inflammatory markers within target tissues was also observed. We were then able to extend these findings by reproducing the anti-cachectic ability of our Fn14-antibodies in the widely studied C-26 mouse model of cancer cachexia. Thus, targeting Fn14 on tumors presents a promising means for treatment of cancer cachexia. The finding that Fn14 is not only involved in wound healing (Winkles, 2008) but also causative of cancer cachexia is consistent with the concept that tumors resemble wounds that do not heal (Dvorak, 1986).

We had specifically chosen antibodies to Fn14 that could antagonize the action of TWEAK, in line with the hypothesis that Fn14-dependent cachexia is caused by an activation of signaling through Fn14. Although in vitro our antibodies can function as antagonists, we cannot rule out that in vivo these anti-cachectic antibodies are operating via Fc-dependent multi-merization pathways. In vitro studies showed the potential of cross-linked Fc domains to reveal agonistic activity (data not shown). This is a common and often desirable feature of antibodies and has been demonstrated for other Fn14 antibodies (Culp et al., 2010; Salzmann et al., 2013).

Combined with the ability of our Fn14 antibody to inhibit cachexia, these observations naturally led to the idea that TWEAK could be the factor that drives muscle wasting in these cancer-induced cachexia models, given that it is the only ligand reported for Fn14 to date. However, the MEF tumors induced cachexia to the same degree in both *Fn14*$^{-/-}$ and *Tweak*$^{-/-}$ mice, which is inconsistent with this hypothesis. Additionally, our data also demonstrated that TWEAK blockade (using a blocking TWEAK antibody) had no effect on the Fn14-induced cachexia, which raises the question of how Fn14 is inducing

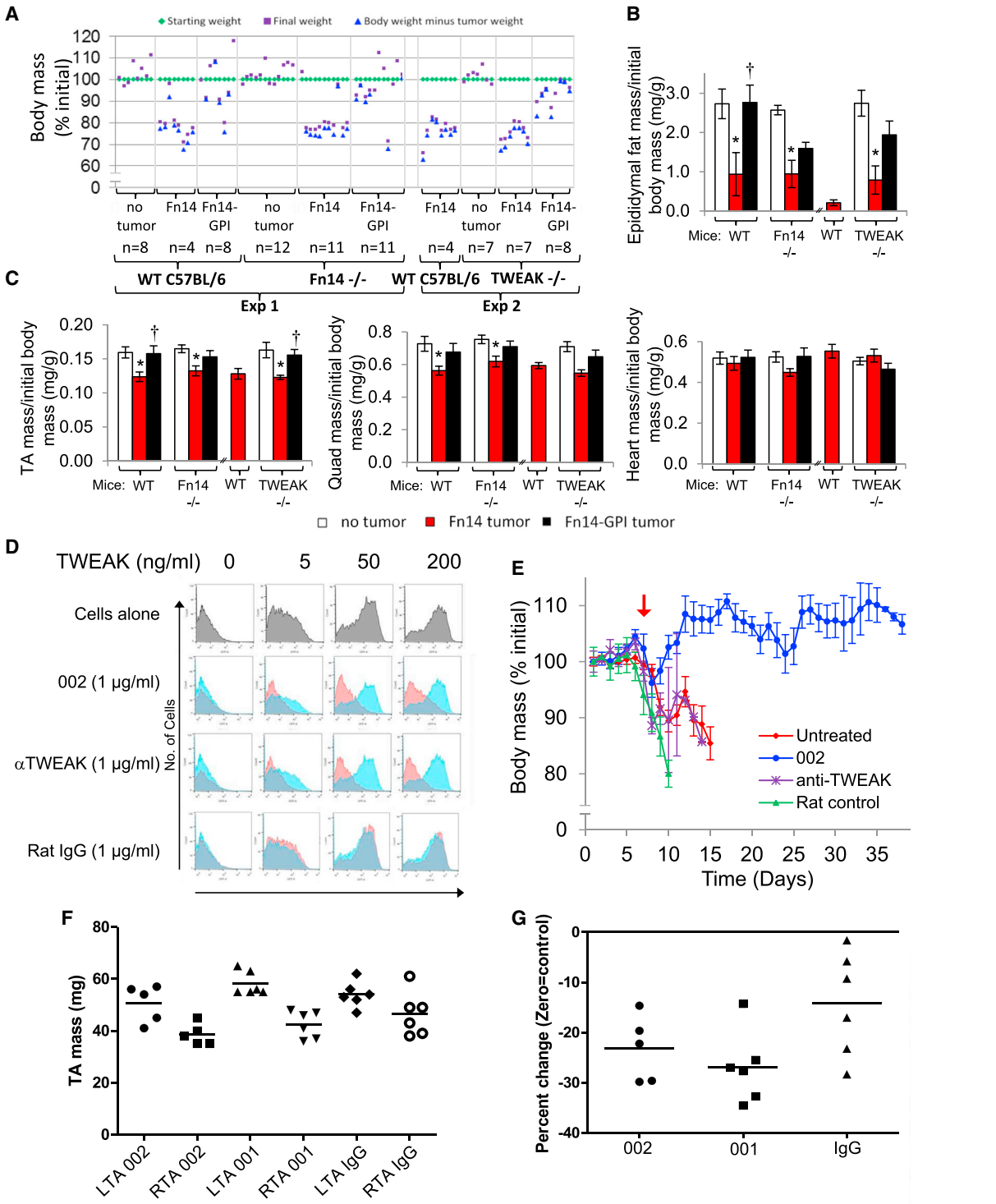

Figure 7. Host Fn14 and TWEAK Are Not Involved in Cachexia

Wild-type, *Fn14*$^{-/-}$ or *Tweak*$^{-/-}$ mice were injected with MEF H-Ras V12 Fn14 or Fn14-GPI tumor cells (day 1).

(A) Starting and final weight and final body weight minus tumor mass, standardized to starting weight. Exp 1 and Exp 2: experiments 1 and 2, respectively. See also Figure S5.

(B and C) Group average (B) epididymal fat and (C) muscle (TA, quadriceps, and heart) standardized against starting body weight. In graphs, double forward slash (//) denotes data obtained in two separate experiments. *$p < 0.05$ versus non-tumor for that strain; †$p < 0.05$ versus Fn14 tumor for that strain. Data are means ± SEM.

(legend continued on next page)

cachexia in a ligand-independent fashion. Ligand-independent receptor multi-merization has been suggested for Fn14 by others as a possibility for pathway activation; however, this idea has stemmed from in vitro overexpression data (Brown et al., 2003; Han et al., 2003), and no in vivo physiological evidence exists to support this hypothesis. Although speculative, another possibility is the presence of a second unidentified ligand for Fn14. Although the mechanism remains unclear, there is no doubt that tumor-localized Fn14 induces cachexia in the models presented here, and antibody therapy ablates this condition.

In addition to its effects during tumorigenesis, Fn14 signaling (via the action of TWEAK) has been linked to inhibiting differentiation of myoblast to muscle (Dogra et al., 2006; Girgenrath et al., 2006) and promoting myoblast proliferation in the presence of TWEAK. In vivo studies using Fn14 or TWEAK knockout and TWEAK transgenic mice support the idea that regulating myogenesis and muscle repair are physiological functions of the TWEAK/Fn14 signaling axis (Tajrishi et al., 2014; Girgenrath et al., 2006; Mittal et al., 2010a, 2010b). Our data from both *Fn14*$^{-/-}$ or *Tweak*$^{-/-}$ mice, as well as a blocking TWEAK antibody, demonstrated that, at least in the models presented here, neither TWEAK nor Fn14 in muscle cells are involved in inducing muscle atrophy pathways directly. This raises the question of why Fn14 expression is increased in muscle during atrophy, and we speculate that this could be in a regenerative capacity. Supportive of such a hypothesis, Fn14 is required for the self-renewal of muscle progenitor cells, and Fn14 knockout mice display delayed muscle regeneration following injury (Girgenrath et al., 2006). In addition to our data generated from cancer-cachexia models, the model for activin A overexpression in muscle promotes upregulation of muscle Fn14 during muscle wasting. Fn14 antibody treatment did not prevent activin A-induced muscle loss, and in fact antibody treatment led to marginally smaller muscle mass than that in control-treated mice, again supporting the hypothesis of Fn14 functioning in a regenerative capacity.

Given that our data argues against the possibility that tumor-derived TWEAK is the causative factor in cancer cachexia and also against muscle atrophy being induced by signaling via localization of Fn14 in the muscle itself, this raises the question of the nature of the soluble factor produced by the tumor that relays the signal to distal tissues. Potential candidates for such signaling molecules could be activins or myostatin because cachexia induced by C-26 tumors was prevented by a decoy activin receptor (ActRIIb) that inhibits activin/myostatin signaling. Interestingly, although muscle wasting caused by C-26 tumors was successfully prevented by the ActRIIb decoy receptor, fat loss, another feature of cachexia, was unaffected (Zhou et al., 2010). In contrast, we have shown that anti-Fn14 treatment of C-26 cachectic animals prevented tumor-induced inflammation, fat loss, and reduction in muscle mass and function. Minimally we can conclude that if activin functions downstream of tumor Fn14 to induce cachexia, it is only one of the components produced by Fn14 tumors. Fn14 is therefore an attractive therapeutic target because it is not required for normal development and is generally absent in normal tissue yet increased in tumors.

Our data implicated tumor Fn14 as an inducer of cachexia in mice models, and therefore translation of these findings to humans was crucial. Cachectic mice lose weight very rapidly, whereas in human cancer patients, cachexia usually progresses slowly, with an average loss of 5% body mass over 12 months. In murine tumor models, the tumor can account for as much as 10% of the total mouse weight; in humans, tumor mass as a proportion of body weight rarely exceeds 1%. Mice also have a different metabolism than humans. Despite the need to be cautious when translating results from mouse models to humans, it is noteworthy that in our experiments similarly sized tumors caused very different cachectic effects. This demonstrates that cachexia is an active, independent process with the tumor directly driving the loss of muscle and fat.

Cancer cachexia has been estimated to be as high as 80% of all cancer cases (Wallengren et al., 2013), and cachexia has been attributed to a patient's inability to tolerate intensive treatment regimens (Argilés et al., 2009; Murphy and Lynch, 2009). Unfortunately, current databases are remarkably deficient concerning the presence of cachexia or its contribution to patient well-being and survival. Even so, our TCGA database analysis promisingly revealed positive correlations between many inflammatory cytokines implicated in cancer cachexia and Fn14 transcripts in patients. The typical lack of diagnosis of cachexia in patient cohorts means, however, that the data cannot directly address whether Fn14 expression plays a role in cachexia.

A therapy that directly targets cancer-associated cachexia is desperately needed. We have demonstrated that anti-Fn14 reagents present a tangible treatment and must now be tested for their efficacy in cancer patients presenting with hallmarks of cachexia. Prior to this, however, there is a pressing and urgent need to generate patient sample data that acknowledge and record central components to cachexia.

EXPERIMENTAL PROCEDURES

Monoclonal Antibody Generation—Immunization of Mice, Hybridoma Production, and Purification

Recombinant Fn14-Fc (Amgen) was used for immunizations. Female Balb/c mice were immunized intraperitoneally (i.p.) with 15 μg of antigen emulsified in Complete Freund 's adjuvant (Sigma). Incomplete Freund's adjuvant was used for subsequent boosts performed at 4 week intervals and final i.p. injection 3 days before spleen removal.

(D) Flow cytometric analysis of HEK293T NF-κB GFP reporter assay. MTW-1 (anti-TWEAK), Rat IgG control, or antibody 002 (red) ± 0–200 ng/ml Fc-TWEAK (gray and blue underlay).

(E) Standardized group body weight of C57BL/6 mice injected with MEF H-Ras V12 Fn14 tumor cells (day 1) and antibody treated (anti-TWEAK MTW-1, control IgG, or 002; day 7; 10 mg/kg; ↓). Data are means ± SEM (n = 8).

(F) Absolute mass values for TA muscles injected with activin-expressing AAV vectors (right TA, RTA) or control vector (left TA, LTA); mice treated with 001, 002, or IgG control.

(G) Percentage change in TA muscle mass, injected with activin-expressing AAV vectors, compared with contralateral muscles receiving control vector.

Hybridoma fusions with SP20 cells were performed using ClonaCell-HY Hybridoma Kit (StemCell Technologies, Inc.). Selection and cloning steps were performed on methylcellulose-based semi-solid media in 96-well plates.

Antibody accumulated from hybridomas grown in serum-free conditioned medium and purified with Protein A Sepharose HiTrap MabSelect Xtra (GE Healthcare). Neutralized eluate from Protein A was concentrated and buffer exchanged with PBS using a vivaspin 20 column (Sartorius). All antibodies had endotoxin < 0.05 EU/mg, determined using Charles River Endosafe PTS.

Antibody Isotyping and Antibodies

Antibodies were isotyped using the BD Cytometric Bead Array. ITEM1, IgG2b, IgG1, and TWEAK (MTW-1); rat IgG1 (Biolegend); anti-VSV (Sigma); anti-HA (made in-house); and AlexaFluor-647 secondary (Invitrogen) were used.

Generation of Constructs and Cell Lines

The 4-hydroxytamoxifen (4-OHT) inducible lentiviral vector previously described (Vince et al., 2007) was used to express human Fn14, or the Fn14 extracellular region fused to the TrailR3 GPI (Bossen et al., 2006), to create Fn14-GPI. Wild-type C57BL/6 MEFs were immortalized with a lentiviral SV40 Large T construct and transformed with a retroviral H-Ras V12 construct. This cell line was then transduced for expression of GEV16 and either Fn14 or Fn14-GPI. One hundred nanomolar 4-OHT was used for protein induction.

Transfections and Western Blotting

HEK293T cells were transiently transfected with DNA encoding TNFRSF members (Bossen et al., 2006) using Lipofectamine 2000. At 24 hr, cells were harvested and lysed in RIPA buffer. Inducible cell lines were grown to ~50% confluency, and Fn14 expression induced for 48 hr. Cells were harvested, washed, and resuspended in 20 mM Tris, pH 7.4, 10 μg/ml DNase1 and RNaseA. Genomic DNA from lysed cells was sheared (27G insulin syringe), samples centrifuged, supernatant collected, and further centrifuged. The pellet was resuspended in 1M Tris, 0.4% SDS, and proteins were separated by reducing SDS-PAGE and western blotted. HRP-conjugated secondary goat anti-mouse was used for detection.

Flow Cytometry

Cells (1×10^5) were incubated with antibody, washed, and stained with AlexaFluor-647-conjugated goat anti-mouse IgG, and flow cytometry was performed with a BD FACSCanto II. Data analysis was done with FlowJo. Fn14 expression was induced 24 hr prior.

HEK293T NF-κB GFP Assay

HEK293T cells containing a stably integrated lentiviral vector and an NF-κB promoter driving GFP (pTRH1 System Biosciences) were incubated for 24 hr ± Fc-TWEAK (5, 50, 100, or 200 ng/ml), ± antibodies. GFP fluorescence was measured by flow cytometry.

Kym1 Cell-Death Assay

Kym1 cell-death assays were performed as described (Vince et al., 2008). Briefly, 24 hr after TWEAK stimulation, live and dead cells were harvested, stained with PI, and analyzed by flow cytometry.

Tumor Cell Lines and Tumor Studies

Two independent sources of C-26 cells from Cell Line Services (Germany) (Figure 4) and a gift from Martha Belury (Ohio State University, Columbus, OH, USA) (Figures 5 and 6) were used; LLC were sourced from European Collection of Cell Cultures. Cells were cultured in 10% DMEM (MEF and LLC) or 10% RPMI (C-26). Mice were obtained from Animal Resources Centre (Canning Vale, Western Australia) or Monash Animal Services (Victoria), and all experiments were approved by the relevant Animal Ethics Committees from La Trobe University (AEC 13-52, 10-54, 11-37, and 10-19B), University of Melbourne (AEC 1112069), or the Alfred Medical Research and Education Precinct (AEC E/1289/2012/B). Tumor measurements were taken using digital calipers, and volume calculated (length × width^2)/2. Pair feeding was achieved by monitoring food intake of 'untreated' tumor group each 24 hr and providing the pair-fed group with that amount of food for the following 24 hr period. Mice received subcutaneous (s.c.) injection of PBS ± 5×10^5–5×10^6 cells on experiment day 1 using an insulin syringe. Antibodies were administered by i.p. injection.

Grip-Strength Test

Whole-body strength was assessed on day 21 using a grip-strength meter (Columbus Instruments, Columbus, OH, USA) as described (Murphy et al., 2012).

Assessment of Functional Properties of TA Muscles

On day 22 (C-26 study) or day 11 (MEF study), mice were anesthetized with sodium pentobarbitone (i.p.; Nembutal; 60 mg/kg), and the contractile properties of the mouse TA muscle assessed (Murphy et al., 2010).

Skeletal Muscle Histology

Serial sections (5 μm) cut transversely through the TA muscle using a refrigerated (−20°C) cryostat (CTI Cryostat; IEC, Needham Heights, MA, USA). Sections were reacted with the following: laminin (Sigma-Aldrich) for mean myofiber cross-sectional area (CSA); SDH for oxidative enzyme activity; and N2.261 (developed by Dr Helen Blau, obtained from the Developmental Studies Hybridoma Bank) for percentage myosin IIa isoforms (Murphy et al., 2010). Digital images were obtained using an upright microscope (Axio Imager D1, Carl Zeiss, Göttingen, Germany), controlled and quantified by AxioVision AC software (Carl Zeiss).

Real-Time PCR Analyses

Total RNA was extracted from 10–20 mg TA muscle using a PureLink RNA Mini Kit (Invitrogen). RNA was transcribed into cDNA using the Invitrogen SuperScript VILO cDNA Synthesis Kit. Real-Time PCR with primers for MuRF-1, atrogin-1, IL-6, and TNF was performed (Murphy et al., 2010). Single-stranded DNA (ssDNA) content in each sample was determined using Quanti-iT OliGreen ssDNA Assay Kit (Molecular Probes, Eugene, OR, USA). Gene expression was quantified by normalizing logarithmic cycle threshold (CT) value (2^{-CT}) to cDNA content of each sample to obtain the expression 2^{-CT}/cDNA content (ng.ml^{-1}).

Activin A Model of Muscle Atrophy

AAV vectors carrying activin A expression cassette, or control AAV, were injected at a dose of 1×10^9 vector genomes into TA muscles of ~8-week-old male isoflurane anaesthetized C57BL/6 mice, as described (Chen et al., 2014). Randomly assigned cohorts received a total of six antibody injections over 4 weeks beginning 4 days after AAV vector injection. TA muscles from both hindlimbs were excised at the experimental endpoint.

SUPPLEMENTAL INFORMATION

Supplemental Information includes Supplemental Experimental Procedures and seven figures and can be found with this article online at http://dx.doi.org/10.1016/j.cell.2015.08.031.

AUTHOR CONTRIBUTIONS

Monoclonal antibodies: D.L., A.J.J., L.J., V.L., K.E., T.S., H.D., J.H., G.T., P.F., N.J.H., and A.M.S. Design/creation of Fn14-expressing tumor model: W.W.-L.W., A.J.J., J. Silke, and L.J. Mouse experiments: L.J., A.J.J., D.L., K.M.J., R.W., H.A., P.F., and J.H. Constructs/cell lines: A.J.J., L.J., M.T., and P.S. Cachexia characterization/muscle function designed and conducted by G.S.L. and K.T.M. Activin A model experiments designed and conducted by P.G. Epitope mapping: M.F., J.L.C., K.E., J. Schloegel, P.F., and R.W. Flow cytometry: L.J. and D.L. and western blotting L.J. Fn14$^{-/-}$ mice provided by L.C.B. Mouse genotyping: C.H. Human database analysis: S.Y.L. Manuscript preparation: L.J., L.C.B., P.S., P.G., and A.M.S. Project coordination, results interpretation, and manuscript writing: A.J.J., J. Silke, N.J.H., G.S.L., and K.T.M.

ACKNOWLEDGMENTS

We acknowledge financial support from the Cooperative Research Centre for Biomarker Translation and the NHMRC. We thank Timur Naim, Annabel Chee,

and Jennifer Trieu for expert technical assistance. We acknowledge the provision of the activin construct, AAV vectors, and technical assistance by Craig Harrison, Hongwei Qian, and Justin Chen. We also acknowledge Stephen Wilcox for MEF tumor cell line genome DNA sequencing. J. Silke is supported by NHMRC grants #541901 and 1058190. K.T.M. is supported by an NHMRC Career Development Fellowship. P.S. is supported by Swiss National Science Foundation grants. N.J.H., J. Silke, and A.M.S. are supported by an NHMRC Development Grant #1075504. L.C.B. is an employee and stockholder of Biogen, Inc.

Received: April 13, 2015
Revised: April 23, 2015
Accepted: August 13, 2015
Published: September 10, 2015

REFERENCES

Argilés, J.M., Busquets, S., Toledo, M., and López-Soriano, F.J. (2009). The role of cytokines in cancer cachexia. Curr. Opin. Support. Palliat. Care *3*, 263–268.

Bossen, C., Ingold, K., Tardivel, A., Bodmer, J.L., Gaide, O., Hertig, S., Ambrose, C., Tschopp, J., and Schneider, P. (2006). Interactions of tumor necrosis factor (TNF) and TNF receptor family members in the mouse and human. J. Biol. Chem. *281*, 13964–13971.

Brown, S.A., Richards, C.M., Hanscom, H.N., Feng, S.L., and Winkles, J.A. (2003). The Fn14 cytoplasmic tail binds tumour-necrosis-factor-receptor-associated factors 1, 2, 3 and 5 and mediates nuclear factor-kappaB activation. Biochem. J. *371*, 395–403.

Brown, S.A., Hanscom, H.N., Vu, H., Brew, S.A., and Winkles, J.A. (2006). TWEAK binding to the Fn14 cysteine-rich domain depends on charged residues located in both the A1 and D2 modules. Biochem. J. *397*, 297–304.

Burkly, L.C., Michaelson, J.S., and Zheng, T.S. (2011). TWEAK/Fn14 pathway: an immunological switch for shaping tissue responses. Immunol. Rev. *244*, 99–114.

Campbell, S., Michaelson, J., Burkly, L., and Putterman, C. (2004). The role of TWEAK/Fn14 in the pathogenesis of inflammation and systemic autoimmunity. Front. Biosci. *9*, 2273–2284.

Chen, J.L., Walton, K.L., Winbanks, C.E., Murphy, K.T., Thomson, R.E., Makanji, Y., Qian, H., Lynch, G.S., Harrison, C.A., and Gregorevic, P. (2014). Elevated expression of activins promotes muscle wasting and cachexia. FASEB J. *28*, 1711–1723.

Culp, P.A., Choi, D., Zhang, Y., Yin, J., Seto, P., Ybarra, S.E., Su, M., Sho, M., Steinle, R., Wong, M.H., et al. (2010). Antibodies to TWEAK receptor inhibit human tumor growth through dual mechanisms. Clin. Cancer Res. *16*, 497–508.

Dewys, W.D., Begg, C., Lavin, P.T., Band, P.R., Bennett, J.M., Bertino, J.R., Cohen, M.H., Douglass, H.O., Jr., Engstrom, P.F., Ezdinli, E.Z., et al.; Eastern Cooperative Oncology Group (1980). Prognostic effect of weight loss prior to chemotherapy in cancer patients. Am. J. Med. *69*, 491–497.

Dogra, C., Changotra, H., Wedhas, N., Qin, X., Wergedal, J.E., and Kumar, A. (2007). TNF-related weak inducer of apoptosis (TWEAK) is a potent skeletal muscle-wasting cytokine. FASEB J. *21*, 1857–1869.

Dogra, C., Changotra, H., Mohan, S., and Kumar, A. (2006). Tumor necrosis factor-like weak inducer of apoptosis inhibits skeletal myogenesis through sustained activation of nuclear factor-kappaB and degradation of MyoD protein. J. Biol. Chem. *281*, 10327–10336.

Dvorak, H.F. (1986). Tumors: wounds that do not heal. Similarities between tumor stroma generation and wound healing. N. Engl. J. Med. *315*, 1650–1659.

Galfrè, G., and Milstein, C. (1981). Preparation of monoclonal antibodies: strategies and procedures. Methods Enzymol. *73* (Pt B), 3–46.

Girgenrath, M., Weng, S., Kostek, C.A., Browning, B., Wang, M., Brown, S.A., Winkles, J.A., Michaelson, J.S., Allaire, N., Schneider, P., et al. (2006). TWEAK, via its receptor Fn14, is a novel regulator of mesenchymal progenitor cells and skeletal muscle regeneration. EMBO J. *25*, 5826–5839.

Han, S., Yoon, K., Lee, K., Kim, K., Jang, H., Lee, N.K., Hwang, K., and Young Lee, S. (2003). TNF-related weak inducer of apoptosis receptor, a TNF receptor superfamily member, activates NF-kappa B through TNF receptor-associated factors. Biochem. Biophys. Res. Commun. *305*, 789–796.

Islam-Ali, B.S., and Tisdale, M.J. (2001). Effect of a tumour-produced lipid-mobilizing factor on protein synthesis and degradation. Br. J. Cancer *84*, 1648–1655.

Kamata, K., Kamijo, S., Nakajima, A., Koyanagi, A., Kurosawa, H., Yagita, H., and Okumura, K. (2006). Involvement of TNF-like weak inducer of apoptosis in the pathogenesis of collagen-induced arthritis. J. Immunol. *177*, 6433–6439.

Macciò, A., Madeddu, C., and Mantovani, G. (2012). Current pharmacotherapy options for cancer anorexia and cachexia. Expert Opin. Pharmacother. *13*, 2453–2472.

Mittal, A., Bhatnagar, S., Kumar, A., Lach-Trifilieff, E., Wauters, S., Li, H., Makonchuk, D.Y., Glass, D.J., and Kumar, A. (2010a). The TWEAK-Fn14 system is a critical regulator of denervation-induced skeletal muscle atrophy in mice. J. Cell Biol. *188*, 833–849.

Mittal, A., Bhatnagar, S., Kumar, A., Paul, P.K., Kuang, S., and Kumar, A. (2010b). Genetic ablation of TWEAK augments regeneration and post-injury growth of skeletal muscle in mice. Am. J. Pathol. *177*, 1732–1742.

Murphy, K.T., Koopman, R., Naim, T., Leger, B., Trieu, J., Ibebunjo, C., and Lynch, G.S. (2010). Antibody-directed myostatin inhibition in 21-mo-old mice reveals novel roles for myostatin signaling in skeletal muscle structure and function. FASEB J. *24*, 4433–4442.

Murphy, K.T., and Lynch, G.S. (2009). Update on emerging drugs for cancer cachexia. Expert Opin. Emerg. Drugs *14*, 619–632.

Murphy, K.T., Chee, A., Trieu, J., Naim, T., and Lynch, G.S. (2012). Importance of functional and metabolic impairments in the characterization of the C-26 murine model of cancer cachexia. Dis. Model. Mech. *5*, 533–545.

Muscaritoli, M., Anker, S.D., Argilés, J., Aversa, Z., Bauer, J.M., Biolo, G., Boirie, Y., Bosaeus, I., Cederholm, T., Costelli, P., et al. (2010). Consensus definition of sarcopenia, cachexia and pre-cachexia: joint document elaborated by Special Interest Groups (SIG) "cachexia-anorexia in chronic wasting diseases" and "nutrition in geriatrics". Clin. Nutr. *29*, 154–159.

Nakayama, M., Ishidoh, K., Kojima, Y., Harada, N., Kominami, E., Okumura, K., and Yagita, H. (2003). Fibroblast growth factor-inducible 14 mediates multiple pathways of TWEAK-induced cell death. J. Immunol. *170*, 341–348.

Russell, S.T., and Tisdale, M.J. (2005). The role of glucocorticoids in the induction of zinc-alpha2-glycoprotein expression in adipose tissue in cancer cachexia. Br. J. Cancer *92*, 876–881.

Salzmann, S., Seher, A., Trebing, J., Weisenberger, D., Rosenthal, A., Siegmund, D., and Wajant, H. (2013). Fibroblast growth factor inducible (Fn14)-specific antibodies concomitantly display signaling pathway-specific agonistic and antagonistic activity. J. Biol. Chem. *288*, 13455–13466.

Schneider, P., Schwenzer, R., Haas, E., Mühlenbeck, F., Schubert, G., Scheurich, P., Tschopp, J., and Wajant, H. (1999). TWEAK can induce cell death via endogenous TNF and TNF receptor 1. Eur. J. Immunol. *29*, 1785–1792.

Tajrishi, M.M., Zheng, T.S., Burkly, L.C., and Kumar, A. (2014). The TWEAK-Fn14 pathway: a potent regulator of skeletal muscle biology in health and disease. Cytokine Growth Factor Rev. *25*, 215–225.

Tisdale, M.J. (2009). Mechanisms of cancer cachexia. Physiol. Rev. *89*, 381–410.

Varfolomeev, E., Blankenship, J.W., Wayson, S.M., Fedorova, A.V., Kayagaki, N., Garg, P., Zobel, K., Dynek, J.N., Elliott, L.O., Wallweber, H.J., et al. (2007). IAP antagonists induce autoubiquitination of c-IAPs, NF-kappaB activation, and TNFalpha-dependent apoptosis. Cell *131*, 669–681.

Varfolomeev, E., Goncharov, T., Maecker, H., Zobel, K., Kömüves, L.G., Deshayes, K., and Vucic, D. (2012). Cellular inhibitors of apoptosis are global

regulators of NF-κB and MAPK activation by members of the TNF family of receptors. Sci. Signal. *5*, ra22.

Vince, J.E., and Silke, J. (2006). TWEAK shall inherit the earth. Cell Death Differ. *13*, 1842–1844.

Vince, J.E., Wong, W.W., Khan, N., Feltham, R., Chau, D., Ahmed, A.U., Benetatos, C.A., Chunduru, S.K., Condon, S.M., McKinlay, M., et al. (2007). IAP antagonists target cIAP1 to induce TNFalpha-dependent apoptosis. Cell *131*, 682–693.

Vince, J.E., Chau, D., Callus, B., Wong, W.W., Hawkins, C.J., Schneider, P., McKinlay, M., Benetatos, C.A., Condon, S.M., Chunduru, S.K., et al. (2008). TWEAK-FN14 signaling induces lysosomal degradation of a cIAP1-TRAF2 complex to sensitize tumor cells to TNFalpha. J. Cell Biol. *182*, 171–184.

Wallengren, O., Lundholm, K., and Bosaeus, I. (2013). Diagnostic criteria of cancer cachexia: relation to quality of life, exercise capacity and survival in unselected palliative care patients. Support. Care Cancer *21*, 1569–1577.

Walsh, D., Donnelly, S., and Rybicki, L. (2000). The symptoms of advanced cancer: relationship to age, gender, and performance status in 1,000 patients. Support. Care Cancer *8*, 175–179.

Warren, S. (1932). The immediate cause of death in cancer. Am. J. Med. Sci. *184*, 610–613.

Wiley, S.R., Cassiano, L., Lofton, T., Davis-Smith, T., Winkles, J.A., Lindner, V., Liu, H., Daniel, T.O., Smith, C.A., and Fanslow, W.C. (2001). A novel TNF receptor family member binds TWEAK and is implicated in angiogenesis. Immunity *15*, 837–846.

Winkles, J.A. (2008). The TWEAK-Fn14 cytokine-receptor axis: discovery, biology and therapeutic targeting. Nat. Rev. Drug Discov. *7*, 411–425.

Zhou, X., Wang, J.L., Lu, J., Song, Y., Kwak, K.S., Jiao, Q., Rosenfeld, R., Chen, Q., Boone, T., Simonet, W.S., et al. (2010). Reversal of cancer cachexia and muscle wasting by ActRIIB antagonism leads to prolonged survival. Cell *142*, 531–543.